

**Determination and analysis of dispersive optical constant
of as deposited and annealed FeS₂ thin films.**

Received : 23\12\2014

Accepted : 8\2\2015

Abdulgussain Abbas Khadayeir

AL- Qadisiya University, College of Education, Physics Department

E-mail. aahussaink@yahoo.com

Abstract

Films of FeS₂ were prepared by the spray pyrolysis technique onto a substrate heated up 350 °C using iron chloride FeCl₂ and thiourea CS(NH₂)₂ solutions with a concentration of 0.1 M. The optical properties of the films were studied using optical absorption measurements in the wavelength range 300-900 nm and confirmed that the annealing temperature has a significant effect on the properties of these films. The optical constants confirm that FeS₂ films have an indirect band gap that decreased from 2.1 to 1.95 eV as the annealing temperature increases to 450°C. The dispersion of the refractive index was analyzed using the concept of a single oscillator. The values of oscillator energy E_o were 4.2, 4, and 3.9eV. The dispersion energy E_d were determined to be 52.7, 90.7, and 102.6 eV for the as deposited films and the annealed films at 400 and 450°C, respectively. The increase in the density of localized states E_d causes an expanding in the Urbach tail and consequently decreases the energy gap.

Keywords: Iron pyrite FeS₂, Optical dispersion parameters, Optical energy gap, Spray pyrolysis.

Physics classification : QC 170-197

Introduction

As a semiconducting material, cubic system iron pyrite FeS₂ has received growing attention due to its promising potential for applications as a photovoltaic or optoelectronic material required to have excellent environment compatibility, excellent electron mobility, high optical absorption coefficient, suitable energy band gap, high quantum efficiency and low production cost for photocurrent generation ^[1-7]. These characteristics made the material to be a promising candidate as an absorber material in thin film solar cells. Synthetic pyrite has been considered to be a more available product than natural ones due to the considerable variety difference and high impurity concentration in the latter. In general, synthetic pyrite can be employed as thin film status since it has high ability of optical absorption.

Many techniques were used to produce pyrite films and the effects of the preparation processes on the structural, stoichiometrical, electrical and optical characteristics have been

reported [8-17]. A complex mechanism was proposed to be responsible for the growth of pyrite films from the iron conversion in sulfur atmosphere or H_2S [18]. Fe_xS or Fe_{1-x}S was first formed chemoepitaxially and then converted into FeS_2 by a chemoendotaxial reaction with sulfur. Grain boundaries played a decisive role in the growth process. The transformation of iron into pyrite was accompanied by a large increase in electrical resistivity during the changes of structure and stoichiometry [19].

In a review of literatures, it can be seen that the effect of annealing parameters on the film characteristics should be studied more sufficiently. In this paper, we report and discuss the characterization of the pyrite films prepared by spray pyrolysis technique and annealed to 400 and 450°C.

Experimental details

Iron pyrite FeS_2 thin films were deposited by the spray pyrolysis technique [20], using iron chloride FeCl_2 (purity: 99.99%) from Sigma-Aldrich UK and thiourea $\text{CS}(\text{NH}_2)_2$ (purity: 99.98%) from Merck Germany. The molarity of the prepared solution is 0.1 M. The FeCl_2 was dissolved in a mixture of methanol and redistilled water in the ratio of 1:1, while the thiourea was dissolved in deionized water. To enhance the solubility of FeCl_2 , a few drops of HCl were also added. The prepared solutions of iron chloride and thiourea were appropriately mixed to obtain an Fe:S proportion of 1:2. The solutions obtained were pulverized on glass substrates with compressed air that maintained at a pressure of 10^5 Nm^{-2} at a flow rate of 5 ml/min and deposition time 5 Sec followed by 2 minutes wait to avoid excessive cooling. The substrate temperature was maintained at 400 °C. The distance from the spray nozzle to the heater was kept at approximately at 29 cm. Under these deposit conditions, good films are obtained. They are uniform and very adherent to the substrates.

The samples were weighed before and after spraying to determine the mass of the films [21]. Knowing the dimensions of the substrates used, the thicknesses can be determined using the following equation [22]:

$$d = \frac{\Delta m}{\rho_m lL} \dots\dots\dots(1)$$

Where Δm is the difference between the mass after and before spraying, ρ_m is the density, l the width and L the length. Optical transmittance and absorbance were recorded in the wavelength range (300-900 nm) using UV-VIS spectrophotometer (Shimadzu Company Japan). The effect of annealing temperatures on the optical properties was investigated.

Results and discussion

The study of the optical absorption of the investigated pyrite films, particularly the absorption edge has proved to be very useful for elucidation of the electronic structure of these materials. The optical absorption spectra of the tested films with different annealing temperatures are shown in Figure 1. The tested films exhibit strong optical absorption in the wavelength range

($\lambda < 550$ nm) and the absorption coefficients reach approximate constants in the regions of high absorption energy. These results were in a good agreement with that obtained by Liu et al. [23]. Moreover, it can be noticed that the absorbance tends to increase with the increasing of annealing temperature to 450°C.

The tail of the absorption edge is exponential, indicating the presence of localized states in the energy band gap. The amount of tailing can be predicted to a first approximation by plotting the absorption edge data in terms of an equation originally given by Urbach [24]. The absorption edge gives a measure of the energy band gap and the exponential dependence of the absorption coefficient, in the exponential edge region Urbach rule is expressed as [25,26]:

$$\alpha = \alpha_0 \exp(h\nu / E_U) \dots\dots\dots (2)$$

Where α_0 is a constant, E_U is the Urbach energy, which characterizes the slope of the exponential edge. Figure (2) shows Urbach plots of the films. The value of E_U was obtained from the inverse of the slope of $\ln \alpha$ vs. $h\nu$ and is given in Table 1. E_U values change inversely with the optical band gap. The Urbach energy values of the films increase with the increasing of annealing temperature. The increase of E_U suggests that the atomic structural disorder of FeS₂ films increases by increasing annealing temperature. This behavior can result from increasing the concentration of surface defects. It is speculated that surface defects in thinner films could play a more important role in the effect on film properties whereas grain boundary defects in thicker films could play a more important role in the effect on film properties, this result was also confirmed by Liu et. al. [23]. So, this increase leads to a redistribution of states, from band to tail and may be attributed to the improvement of crystallinity of anatase phase. As a result, both a decrease in the optical gap and expanding of the Urbach tail have taken place.

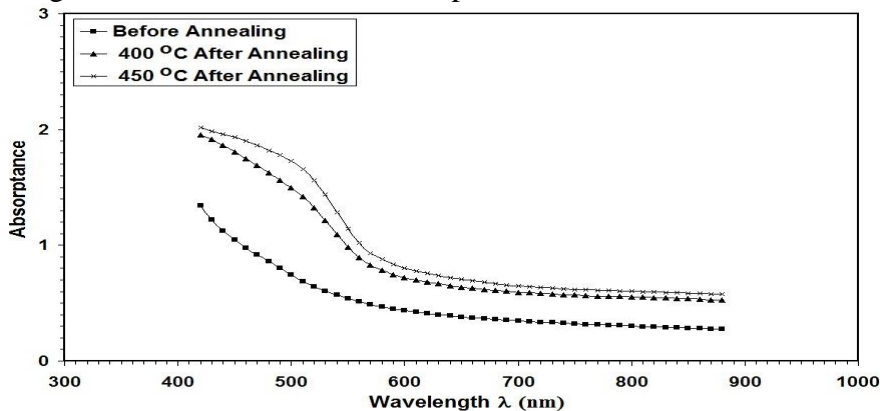


Fig. (1) Absorbance of as deposited and annealed FeS₂ films versus wavelength.

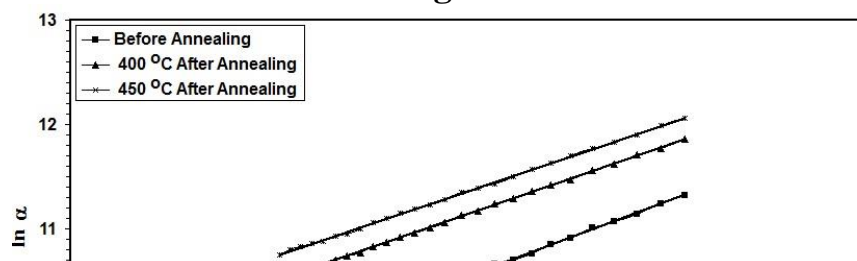


Fig. (2) $\ln\alpha$ versus photon energy for as deposited and annealed FeS₂ films.

According to inter-band absorption theory, the optical band of the FeS₂ films can be calculated using Tauc's relation ^[25]:

$$(\alpha h\nu) = A(h\nu - E_g)^n \dots\dots\dots(3)$$

where α is the absorption coefficient, A a constant, h is Planck's constant, ν the photon frequency, E_g the optical band gap and n is an index which could take different values according to the electronic transition. For allowed direct transitions the coefficient n is equal to 1/2 and for allowing indirect transitions n = 2. The curves $(\alpha h\nu)^{1/2}$ for the allowed direct transition does not present evidence linearity, this seems to suggest that FeS₂ has an indirect band gap.

The value E_g corresponding to the indirect band gap transition was calculated from the curve of $(\alpha h\nu)^2$ versus $h\nu$, using the formula:

$$(\alpha h\nu)^2 = A(h\nu - E_g) \dots\dots\dots(4)$$

The extrapolation of the linear part of the curve $(\alpha h\nu)^2$ to the energy axis is shown in Fig. 3. The indirect band-gap energy of the as deposited film is equal to 2.1eV, this value is in good agreement with the value obtained by Anuar et al. ^[27] (1.85-2.25eV) However, this value is larger than those reported by Wan et al. ^[28] (1.16 eV) and Heras et al. ^[29] (1.05 eV). According to Ben Haj Salah et al. ^[30], the observed disparity in the energy gap is explained by the different growth conditions of these films. It can be seen that the energy band gap of the films tends to decrease to 1.95 eV with increasing annealing temperature to 450°C. Due to the fact that at any temperature crystals contain various structural imperfections or defects “the ideal crystal does not exist”, the decrease in the optical band gap with increasing annealing temperature can be attributed to a decrease in crystallinity disorder of the films. The optical band gap of FeS₂ film is obviously affected by the defects and the crystallinity.

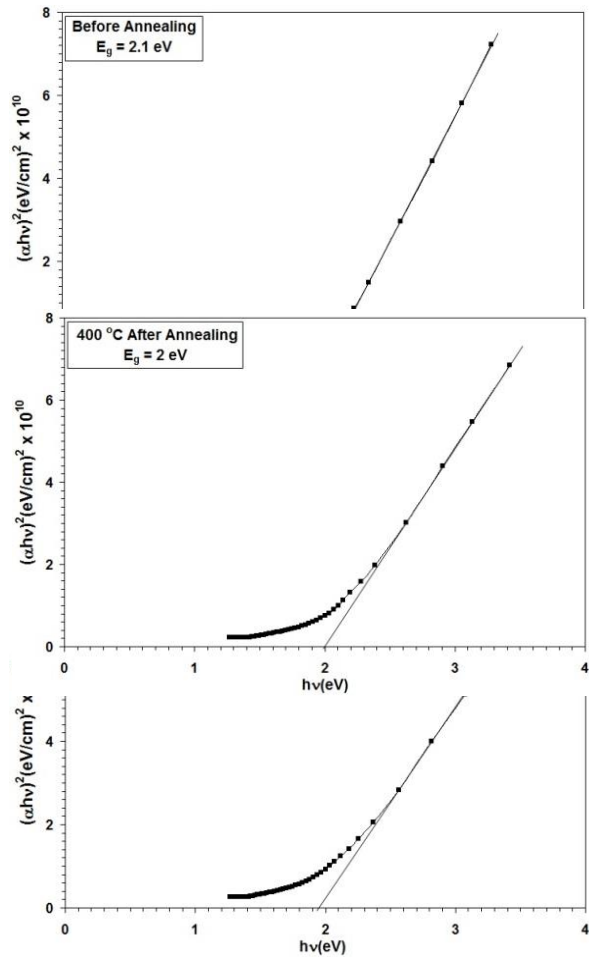


Fig (3) $(\alpha hv)^2$ for FeS₂ film versus photon energy for the as deposited and annealed films.

S. Wemple and H. Didomenico [31,32] use a single-oscillator description to define dispersion energy parameters E_d and E_o . The refractive index dispersion plays an important role in the optical communication and designing of the optical devices. Therefore, it is a significant factor. Although these rules are quite different in detail, one common feature is the over-whelming evidence that both crystal structure and ionicity influence the refractive-index behavior of solids in ways that can be simply described. The relation between the refractive index n , and the single oscillator strength below the band gap is given by the expression:

$$n^2 = 1 + [E_d E_o / E_o^2 - E^2] \dots\dots\dots (5)$$

Where E_d and E_o are single oscillator constants, E_o is the energy of the effective dispersion oscillator, E_d the so-called dispersion energy, which measures the intensity of the inter band optical transitions. The oscillator energy E_o is an average of the optical band gap, E_{opt} , can be obtained from the Wemple–Didomenico model. This model describes the dielectric response for transitions below the optical gap. Experimental verification of Eq. (4) can be obtained by plotting $(n^2-1)^{-1}$ versus $(hv)^2$ as illustrated in Fig. 4 which yields a

straight line for normal behavior having the slope $(E_o E_d)^{-1}$ and the intercept with the vertical axis equal to E_o/E_d . E_o and E_d values were determined from the slope, $(E_o E_d)^{-1}$ and intercept (E_o/E_d) on the vertical axis. E_o values decreased as the optical band gap decreases. According to the single-oscillator model, the single oscillator parameters E_o and E_d are related to the imaginary part of the complex dielectric constant, the moments of the imaginary part of the optical spectrum M_{-1} and M_{-3} moments can be derived from the following relations ^[33]:

$$E_o^2 = M_{-1} / M_{-3} \dots\dots\dots (6)$$

$$E_d^2 = M_{-1}^3 / M_{-3} \dots\dots\dots (7)$$

The values obtained for the dispersion parameters E_o , E_d , M_{-1} and M_{-3} are listed in Table (1). The obtained M_{-1} and M_{-3} moments are increased with increasing the annealing temperature. For the definition of the dependence of the refractive index (n) on the light wavelength (λ), the single-term Sellmeier relation can be used ^[31]:

$$n^2(\lambda) - 1 = S_o \lambda_o^2 / 1 - (\lambda_o/\lambda)^2 \dots\dots\dots (8)$$

Where λ_o is the average oscillator position and S_o is the average oscillator strength. The parameters S_o and λ_o in Eq. (8) can be obtained experimentally by plotting $(n^2 - 1)^{-1}$ versus λ^{-2} as shown in Fig.(5), the slope of the resulting straight line gives $1/S_o$, and the infinite-wavelength intercept gives $1/ S_o \lambda_o^2$. The results shows a decrease in the band gap which may be attributed to the presence of unstructured defects, that increase the density of localized states and cause an expanding in the Urbach tail and consequently decrease the energy gap.

Table (1) The optical parameters

Sample	E_d (eV)	E_o (eV)	E_g (eV)	ϵ_∞	$n(o)$	M_{-1}	M_{-3} eV ⁻²	S_o x10 ¹³ m ⁻²	λ_o nm	U_{tail} meV
Before Annealing	52.7	4.2	2.10	13.5	3.67	12.5	0.71	4.1	553	714
400°C After Annealing	90.7	4.0	2.00	23.0	4.80	22.2	1.33	4.8	642	769
450°C After Annealing	102.6	3.9	1.95	27.0	5.20	26.3	1.73	5.8	660	781

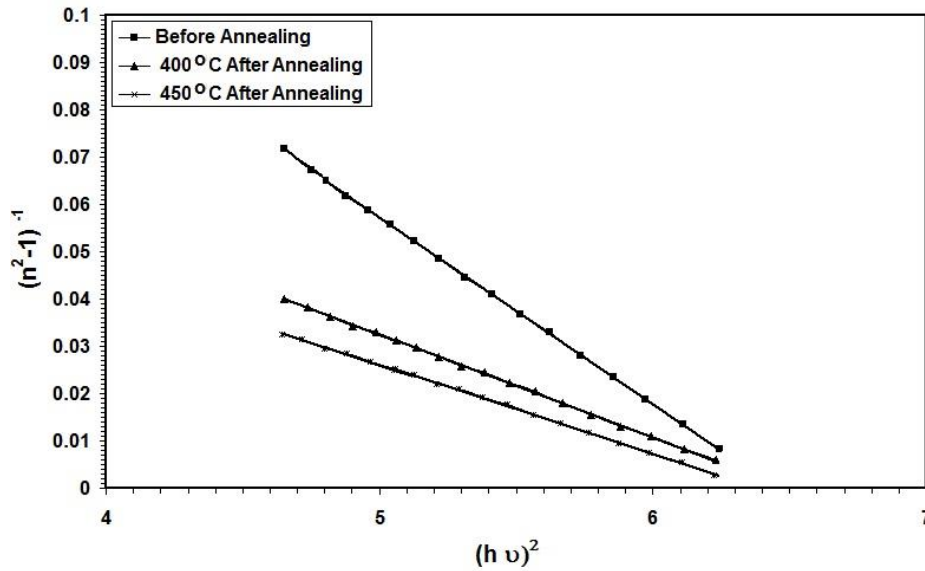


Fig. (4) Variation in $(n^2 - 1)^{-1}$ as a function of $(h\nu)^2$ for FeS₂ films.

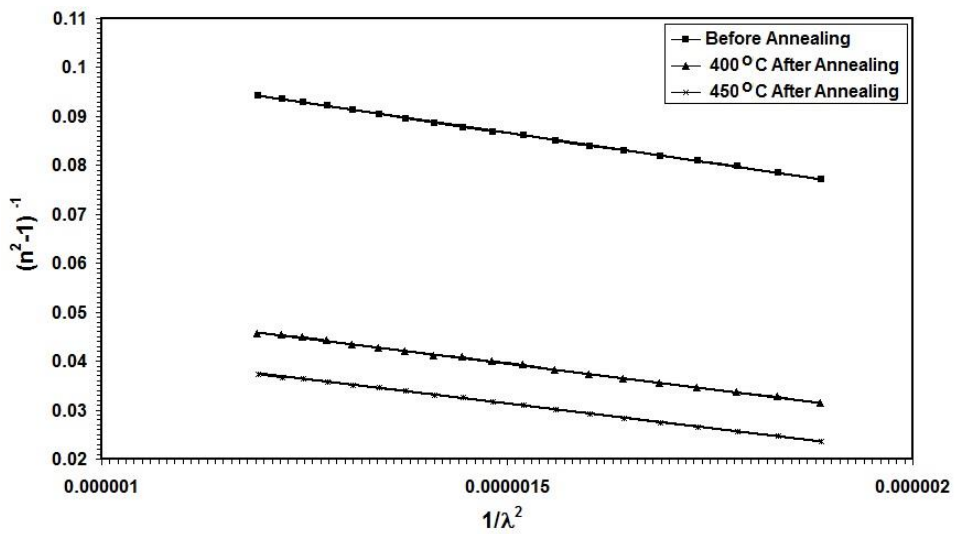


Fig. (5) Variation in $(n^2 - 1)^{-1}$ as a function of $(\lambda)^{-2}$ for FeS₂ films.

Conclusion

Iron pyrite FeS₂ thin films have been successfully deposited onto a glass substrate by the spray pyrolysis technique. The as deposited and annealed films were optically characterized by using UV-VIS technique and the results were systematically presented. The optical band gaps were calculated in terms of Tauc method and Wemple–Didomenico model. The type of optical transition responsible for optical absorption was indirect allowed transitions. The E_g WD values obtained from Wemple–Didomenico model are in agreement with those determined from the Tauc model and found to be decreasing with the increasing of annealing temperature and have the values of 2.1, 2, and 1.95eV for the as deposited, annealed films at 200, and 250°C respectively. The optical dispersion parameters were characterized. The single oscillator parameters were determined. It was shown that the dispersion parameters of the films obeyed the single oscillator model, the change in dispersion was investigated and its value decreased from 4.2 to 3.9 with increasing annealing temperature to 450°C.

References

- [1] K. Bükler, N. Alonso-Vante, and H. Tributsch, "Photovoltaic output limitation of n-FeS₂ (pyrite) Schottky barriers: A temperature-dependent characterization", *J. Appl. Phys.* 72 (1992) 5721-5729. <http://dx.doi.org/10.1063/1.351925>.
- [2] P. P. Altermatt, T. Kiesewetter, K. Ellmer, H. Tributsch, "Specifying targets of future research in photovoltaic devices containing pyrite (FeS₂) by numerical modeling", *Solar Energy Mater. Solar Cells* 72 (2002) 181-195.
- [3] A. Ennaoui, S. Fiechter, Ch. Pettenkofer, N. Alonso-Vante, K. Bükler, M. Bronold, Ch. Höpfner, H. Tributsch, "Iron Disulfide for Solar Energy Conversion", *Solar Energy Mater. Solar Cells* 29 (1993) 289-370.
- [4] I. J. Ferrer, D. M. Nevskaya, C. de las Heras, C. Sánchez, "About the band gap nature of FeS₂ as determined from optical and photoelectrochemical measurements", *Solid State Commun.* 74 (1990) 913-916.
- [5] A. Ennaoui, S. Fiechter, H. Goslowky, H. Tributsch, "Photoactive Synthetic Polycrystalline Pyrite (FeS₂)", *J. Electrochem. Soc.* 132 (1985) 1579-1582. doi: 10.1149/1.2114168.
- [6] I. J. Ferrer, C. Sanchez, "Characterization of FeS₂ thin films prepared by thermal sulfidation of flash evaporated iron", *J. Appl. Phys.* 70 (1991) 2641-2647. <http://dx.doi.org/10.1063/1.349377>
- [7] S. Nakamura, A. Yamamoto, "Electrodeposition of pyrite (FeS₂) thin films for photovoltaic cells", *Solar Energy Mater. Solar Cells* 65 (2001) 79-85.
- [8] L. Meng, Y. H. Liu, W. Huang, "Synthesis of pyrite thin films obtained by thermal-sulfurating iron films at different sulfur atmosphere pressure", *Mater. Sci. Eng. B* 90 (2002) 84-89.
- [9] J. Oertel, K. Ellmer, W. Bohne, J. Röhrich, H. Tributsch, "Growth of n-type polycrystalline pyrite (FeS₂) films by metalorganic chemical vapour deposition and their electrical characterization", *J. Crystal Growth* 198-199 (1999) 1205-1210.
- [10] A. Sanhueza, I. J. Ferrer, T. Vargas, R. Amils, C. Sanchez, "Attachment of Thiobacillus ferrooxidans on synthetic pyrite of varying structural and electronic properties", *Hydrometallurgy* 51 (1999) 115-129.
- [11] B. Thomas, T. Cibik, C. Höpfner, K. Diesner, G. Ehlers, S. Fiechter, K. Ellmer, "Formation of secondary iron-sulphur phases during the growth of polycrystalline iron pyrite (FeS₂) thin films by MOCVD", *J. Mater. Sci.: Mater. in Electronics* 9 (1998) 61-64.
- [12] N. Hamdadou, A. Khelil, J. C. Bernede, "Pyrite FeS₂ films obtained by sulphuration of iron pre-deposited films", *Mater. Chem. Phys.* 78 (2003) 591-601.
- [13] L. Meng, Y. H. Liu, L. Tian, "Structural, optical and electrical properties of polycrystalline pyrite (FeS₂) films obtained by thermal sulfuration of iron films", *J. Crystal Growth* 253 (2003) 530-538.

- [14] A. Yamamoto, M. Nakamura, A. Seki, E. L. Li, A. Hashimoto, S. Nakamura, "Pyrite (FeS₂) thin films prepared by spray method using FeSO₄ and (NH₄)₂Sx", *Solar Energy Mater. Solar Cells* 75 (2003) 451-456.
- [15] Rachel Morrish, Rebecca Silverstein, and Colin A. Wolden, "Synthesis of Stoichiometric FeS₂ through Plasma-Assisted Sulfurization of Fe₂O₃ Nanorods", *J. Am. Chem. Soc.*, 2012, 134 (43) 17854-17857. doi: 10.1021/ja307412e.
- [16] Nafise E'jazi, Mahmoud Aghaziarati, "Determination of optimum condition to produce nanocrystalline pyrite by solvothermal synthesis method", *Advanced Powder Technology* 23 (2012) 352-357.
- [17] A. K. Raturi, S. Waita, B. Aduda, T. Nyangona, "Photoactive iron pyrite films for photoelectrochemical (PEC) cells", *Renewable Energy* 20 (2000) 37-43.
- [18] G. Pimenta, W. Kautek, "Pyrite film formation by H₂S reactive annealing of iron", *Thin Solid Films* 238 (1994) 213-217.
- [19] C. de las Heras, D. Salto, I. J. Ferrer, C. Sánchez, "In situ electrical resistivity measurements during the sulphuration of pyrite and Fe thin films", *J. Phys.: Condens. Matter* 6 (1994) 899-906.
- [20] N. Benramdane, M. Latrache, H. Tabet, M. Boukhalfa, Z. Kebbab, A. Bouzidi, "Structural and optical properties of spray-pyrolysed Bi₂S₃ thin films", *Mater. Sci. Eng. B* 64 (1999) 84-87.
- [21] H. Tabet-Derraz, N. Benramdane, D. Nacer, A. Bouzidi, M. Medles, "Investigations on Zn_xCd_{1-x}O thin films obtained by spray pyrolysis", *Sol. Energy Mater. Sol. Cells* 73 (2002) 249-259.
- [22] M. Medles, N. Benramdane, A. Bouzidi, A. Nakrela, H. Tabet-Derraz, Z. Kebbab, C. Mathieu, B. Khelifa, R. Desfeux, "Optical and electrical properties of Bi₂S₃ films deposited by spray pyrolysis", *Thin Solid Films* Vol. 497 (2006) 58-64.
- [23] Liu Yanhui, Meng Liang, Zhang Lei., "Optical and electrical properties of FeS₂ thin films with different thickness prepared by sulfurizing evaporated iron", *Thin Solid Films* 479, (1-2) (2005) 83-88.
- [24] Urbach F., "The Long-Wavelength Edge of Photographic Sensitivity and of the Electronic Absorption of Solids", *Phys. Rev.*, Vol. 92 (1953) 1324-1325.
- [25] J. Tauc, "Amorphous and Liquid Semiconductors", Plenum Press, New York, 1974.
- [26] J. Tauc, R. Grigorovici, and A. Vancu, "Optical Properties and Electronic Structure of Amorphous Germanium", *Phys. Status Solidi*, 15 (1966) 627-637.
- [27] K. Anuar, W.T. Tan, N. Saravanan, S.M. Ho, and S.Y. Gwee, "Influence of pH Values on Chemical Bath Deposited FeS₂ Thin Films", *The Pacific Journal of Science and Technology*, Vol. 10. No. 2 (2009) 801-805. <http://www.akamaiuniversity.us/PJST.htm>
- [28] Dongyun Wana, Yutian Wanga, Baoyi Wanga, Chuangxin Maa, Hong Sunb, Long Weia, "Effects of the crystal structure on electrical and optical properties of pyrite FeS₂ films prepared by thermally sulfurizing iron films", *Journal of Crystal Growth* 253 (2003) 230-238.
- [29] C de las Heras, I J Ferrer and C Sanchez, "Temperature dependence of the optical absorption edge of pyrite FeS₂ thin films", *Journal of Physics: Condensed Matter* Vol. 6 (1994) 10177-10183. doi:10.1088/0953-8984/6/46/033
- [30] H. Ben Hadj Salah, H. Bouzouita, B. Rezig, "Preparation and characterization of tin sulphide thin films by a spray pyrolysis technique", *Thin Solid Films* 480-481 (2005) 439-442.
- [31] Wemple, S. H., DiDomenico, "Oxygen - Octahedra Ferroelectrics I. Theory of Electro-Optical and Non Linear Optical Effects", *J. Appl. Phys.*, 40 (2) (1969) 720-734.
- [32] Wemple, S. H., DiDomenico, "Behavior of the Electronic Dielectric Constant in Covalent and Ionic Materials", *Phys. Rev.*, B3 (1971) 1338-1351.
- [33] Atyia, H. E., "Influence of deposition temperature on the structural and optical properties of InSbSe₃ films", *Optoelectron. Adv. M.*, Vol. 8 (2006) 1359-1366.

تحديد وتحليل ثابت التفريق الضوئي لأغشية كبريتيد الحديد الرقيقة المرسبة والملدنه

تاريخ القبول : 2015\2\8

تاريخ الاستلام : 2014\12\23

عبد الحسين عباس خضير
جامعة القادسية – كلية التربية – قسم الفيزياء

الخلاصة

حضرت أغشية كبريتيد الحديد بتقنية الرش الكيميائي الحراري على قواعد زجاجية مسخنة بدرجة حرارة 350°C باستعمال محاليل كلوريد الحديد والثايوريا بنسبة 0.1 مولارية. درست الخصائص البصرية لهذه الأغشية بالاعتماد على قياسات الامتصاصية بمدى الطول الموجي 300-900 nm. اكدت النتائج بان التلدين له تأثير ملحوظ على خصائص هذه الأغشية. اذا اثبتت حسابات الثوابت البصرية ان كبريتيد الحديد يمتلك فجوة طاقة غير مباشرة والتي تقل قيمتها من 2.1 eV الى 1.95 eV بزيادة درجة حرارة التلدين الى 450°C . حلت قيم معامل انكسار التفريق باستعمال مفهوم التذبذب المفرد. ان قيم طاقة التذبذب كانت 4.2, 4, 3.9 eV وطاقة التفريق E_d قد حددت قيمتها 52.7, 90.7, 102.6 eV للأغشية غير الملدنه والملدنه بالدرجات الحرارية 400°C و 450°C . ان الزيادة في كثافة مستويات الطاقة الموضوعية E_d سببه هو التوسع الحاصل في ذبول اورباخ والذي يؤدي الى نقصان في قيم فجوة الطاقة.

كلمات مفتاحية: كبريتيد الحديد، الاعدومات البصرية، فجوة الطاقة البصرية، الرش الحراري.

Physics classification : QC 170-197